J. Ocean Univ. China (Oceanic and Coastal Sea Research)
https://doi.org/10.1007/s11802-023-5343-9
ISSN 1672-5182, 2023 22 (3): 709-716
http://www.ouc.edu.cn/xbywb/
E-mail:xbywb@ouc.edu.cn

Influence of Cathode Modification by Chitosan and Fe^{3+} on the Electrochemical Performance of Marine Sediment Microbial Fuel Cell

ZAI Xuerong1), 2), GUO Man1), 2), HUANG Xiang1), ZHANG Huaijing3), CHEN Yan2),
JI Hongwei2), and FU Yubin1), *

1) *School of Materials Science & Engineering*, *Ocean University of China*, *Qingdao* 266100, *China*
2) *College of Chemistry and Chemical Engineering*, *Ocean University of China*, *Qingdao* 266100, *China*
3) *College of Marine Geosciences*, *Ocean University of China*, *Qingdao* 266100, *China*

(Received January 27, 2022; revised October 8, 2022; accepted November 27, 2022)

Abstract The electrochemical performances of cathode play a key role in the marine sediment microbial fuel cells (MSMFCs) as a long lasting power source to drive instruments, especially when the dissolved oxygen concentration is very low in seawater. A CTS-Fe^{3+} modified cathode is prepared here by grafting chitosan (CTS) on a carbon fiber surface and then chelating Fe^{3+} through the coordination process. The electrochemical performance in seawater and the output power of the assembled MSMFCs are both studied. The results show that the exchange current densities of CTS and the CTS-Fe^{3+} group are 5.5 and 6.2 times higher than that of the blank group, respectively. The potential of the CTS-Fe^{3+} modified cathode increases by 138 mV. The output power of the fuel cell (613.0 mW m^{-2}) assembled with CTS-Fe^{3+} is 54 times larger than that of the blank group (11.4 mW m^{-2}) and the current output corresponding with the maximum power output also increases by 56 times. Due to the valence conversion between Fe^{3+} and Fe^{2+} on the modified cathode, the kinetic activity of the dissolved oxygen reduction is accelerated and the depolarization capability of the cathode is enhanced, resulting higher cell power. On the basis of this study, the new cathode materials will be encouraged to design with the complex of iron ion in natural seawater as the catalysis for oxygen reduction to improve the cell power in deep sea.

Key words marine sediments; microbial fuel cell; chitosan and iron chelation; modified cathode; electrochemical performance; power output

1 Introduction

Ocean exploration and survey require uninterruptible power to drive instruments for long periods. Therefore, a sustainable power supply is the premise and bottleneck for working instruments under the sea (Ewing *et al.*, 2017). However, until now, conventional batteries and electric cables can not satisfy the power supply of un-attendant instruments on the remote ocean floor. Marine sediment microbial fuel cells (MSMFCs), are new electrochemical devices that can convert the chemical energy of organics in sediments into electric power and have been utilized as sustainable power sources to drive small instruments to work for long term (Tender *et al.*, 2008; Zhou *et al.*, 2018). However, the low power output severely limits its further practical application.

The main factors influencing microbial fuel cell performance include the electricity-producing microorganisms (Cheng *et al.*, 2020; Wang *et al.*, 2021), cathode catalysis, electrode material, cell configuration and the operating parameters (Mahmoud *et al.*, 2018; Asim *et al.*, 2020). Currently, research has been mainly focused on the anode modification of MSMFCs to increase the power (Chen *et al.*, 2017; Zhao *et al.*, 2017; Zhang *et al.*, 2018). In contrast, its cathode modifications for marine application are rarely reported (Babauta *et al.*, 2014). Oxygen is the final electron acceptor in non-biological carbon cathodes, for example, carbon paper, carbon cloth or carbon fiber *et al.* However, the dissolved oxygen (DO) concentration in sea water is much lower than the conventional air fuel cells and its reduction rate is also much lower on this type of carbon materials. The transfer rate of electrons between the cathode and dissolved oxygen is the key limiting factor (Choreishi *et al.*, 2014; Yang *et al.*, 2020), and the DO reduction reaction (DORR) could be greatly enhanced by using a catalyst with higher activity.

Typically used catalysts include Pt, transition metals and ferricyanide. Pt metal is currently the ideal electrode catalyst. However, Pt is easily poisoned in sea water and its cost is high, thereby limiting its application. Transition

---

* Corresponding author. Tel: 0086-532-60891690
E-mail: ffyybb@ouc.edu.cn

metals, such as Fe, Mn, Co and its alloys or oxides, could be used as the electron transfer media on the electrode surface (Gajda *et al.*, 2018; Huang *et al.*, 2018; Liu *et al.*, 2018; Zhou *et al.*, 2018). The conversion of metal valence states would accelerate the electron transmission and improve the cathode performance. In recent years, researches on the electrode loaded with catalysis have been increasingly focused on the high efficient oxygen reduction reaction (ORR) (Song *et al.*, 2018).

Chitosan (CTS) is a derivative of chitin by the hydrolysis and partial removal of acetyl groups under alkaline conditions. It has the chemical name β-(1,4)-2-amino-2-deoxidation-*D*-glucose and possesses good biological compatibility. The existence of $-NH_2$ in the CTS structure and the cage-type molecule structure formed by hydrogen bonding provide an excellent coordination capability with metal ions (Jiang *et al.*, 2007; Ge *et al.*, 2018; Son *et al.*, 2018). A number of metal ions (*e.g.*, Fe^{2+}, Fe^{3+} and Cu^{2+}) are found in natural seawater and can be coordinated with ligands and the sequence of the coordination selectivity of CTS compared to the three types of ion is $Cu^{2+} > Fe^{3+} > Fe^{2+}$ (Cavalcanti *et al.*, 2012; Zhang *et al.*, 2015). Some researches focused on the chitosan modified composite electrodes as high performance enzyme immobilized biofuel cell to removal pollutants (Ngoc *et al.*, 2019; Yang *et al.*, 2021). However, few researches have been reported on the chitosan modified cathode in marine sediment microbial fuel cell for higher power harvest.

The cathode surface modification by chelation of CTS with Fe ions will significantly improve the electrochemical performance of the MSMFCs through accelerating the kinetic activity of DO reduction. Herein, CTS and Fe^{3+} ions are introduced on the carbon fiber surface by coordination of CTS with Fe ions to fabricate a novel marine cathode. In the modified MSMFCs, the CTS-Fe^{3+} complex receives electrons to become CTS-Fe^{2+}, which is then oxidized back to a CTS-Fe^{3+} by the dissolved oxygen in seawater. The modified cathode electrochemical activity of the DO reduction in seawater is enhanced and the cell power is greatly improved. This research will aid the design of a high efficiency cathode material suitable for low DO concentration in seawater.

2 Experiment

2.1 Preparation Process of Modified Cathode

1) Pre-treatment of carbon fiber: a carbon fiber brush was placed in the muffle and heat treated at 300℃ for 1 h and then cooled and washed with acetone and distilled water in sequence. 2) Oxidation of carbon fiber brush: the pre-treated carbon fiber brush was placed in 65% concentrated nitric acid and stirred for 2 h at 90℃ and then washed by water until its pH reaches neutral. 3) Grafting of CTS by chemical method: the oxidized carbon fiber brush was immersed in the solution of CTS and acetic acid (0.5 g of CTS and 500 mL of distilled water added with 10% acetic acid until total dissolution and 1 mL pyridine) at 80℃ for 2 h. During the heating process, a NaOH solution of $0.3\,mol\,L^{-1}$ was dripped in and the remaining CTS and pyridine were cleaned at the end of the reaction (Wu *et al.*, 2017). 4) Preparation of CTS-Fe^{3+}-modified cathode: the carbon fiber brush grafted with CTS was immersed in a $3.5\,g\,L^{-1}$ $FeCl_3$ solution with the pH adjusted at 6.5 and then distillated water was used to clean extra Fe ions for 5 h (Ge *et al.*, 2018). Four groups of cathode were prepared as followings: blank, oxidation (O), modification with CTS, chelation modification (CTS-Fe^{3+}). The modification process is shown in Figs.1a and 1b.

(a) Oxidation of carbon fiber

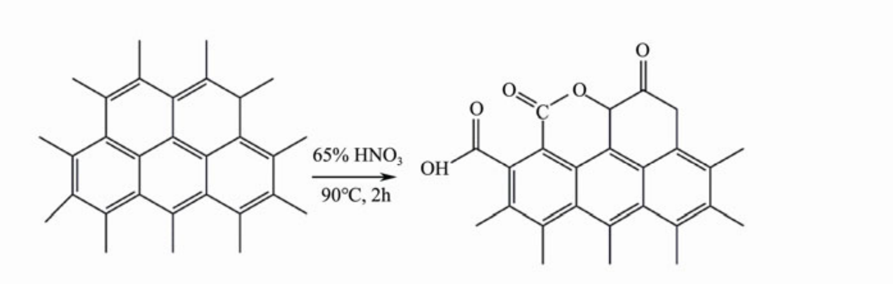

(b) Chitosan graft reaction

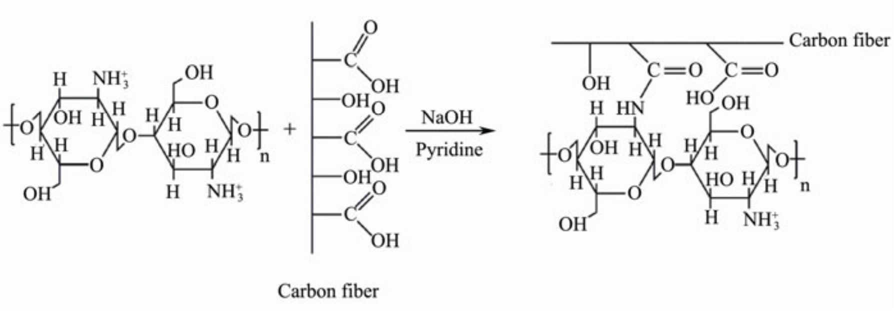

Fig.1 Chitosan modification process on carbon fiber surface. (a), chemical oxidation treatment of carbon fiber; (b), chitosan graft on carbon fiber.

Fourier transfer infrared (FT-IR) spectroscopy was used to characterize the grafted CTS molecular functional groups and scanning electron microscopy (SEM) was utilized to obtain its microscopic patterns on the modified carbon surface. Energy dispersive X-ray spectrometry (EDS) determines its element components after carbon fiber modification.

2.2 Anode Preparation and Cell Construction

As illustrated in Fig.1c, 200 carbon fiber brushes in parallel were adopted for the anode and embedded into the marine sediment in which each carbon fiber brush has a diameter of 5 cm and length of 30 cm, so that the anodic electrochemical performance was maintained at steady state. Five cathode carbon fiber brushes were placed in the natural seawater in the upper layer of the chamber, and a variable resistor was loaded in the external circuit and a cell loop was formed by the wire connection (Fig.2). Marine sediment and seawater were fetched from Jiaozhou Bay, Qingdao, China (36˚18΄N, 120˚31΄E) and utilized directly to construct the MSMFC, in which the MSMFCs directly use natural sea water as medium, not the buffer solution in the conventional microbial fuel cell (MFC).

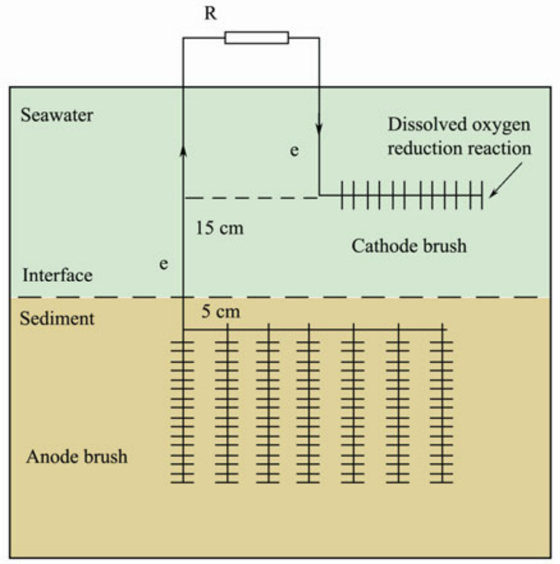

Fig.2 Sketch map of the MSMFC configuration.

2.3 Electrochemical Testing

IM6 electrochemical workstations were applied to test the cyclic voltammetry curve, Tafel curve and electrochemical impedance spectroscopy of the carbon brush cathode, in which, the cathode carbon brush was the working electrode, Pt as the counter electrode and Ag/AgCl as the reference electrode. The scan window of the cyclic voltammetry test was 0.6−0.2 V and the scanning speed 2 mV s^{-1}. The Tafel scanning range was *OCP*±0.2 V and the scanning speed 1 mV s^{-1}. The electrochemical impedance spectroscopy test range was 10 mHz−20 KHz and the amplitude 5 mV.

The power and cathode polarization curve were tested in the three-electrode system by utilizing three multimeters to measure cell current, cell voltage, the anode Ψ_a and cathode potential Ψ_c (mV. *vs*. Ag/AgCl) with continuous adjusting the external resistance method from mega ohm to zero. Following the external ohm decrease, we need to adjust the voltage grade from mV to V, and current grade from mA to A respectively, so that the higher current will cause the multimeter occur clear saltatorial or shoot-back-up values. The obtained current and voltage values were utilized to calculate the maximum power output and to draw cathode polarization curves. Three parallel cell constructions were assembled and parallel tests conducted to obtain average values.

3 Results and Discussion

3.1 Characteristic Analysis of Cathode Surface

3.1.1 FT-IR analysis

The FT-IR results are shown in Fig.3. The chitosan grafted sample showed a N-H stretching vibration peak at 3438 cm^{-1}, while amide I, II and III bands were at 1652, 1580 and 1415 cm^{-1}, respectively. The C-O stretching vibration peak appeared at 1059 cm^{-1}, while the N-H flexural vibration peak was at 644 cm^{-1}.

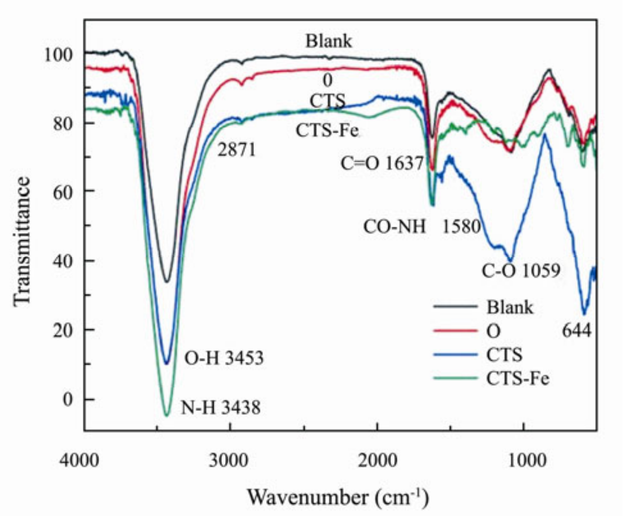

Fig.3 FT-IR spectra for different cathode materials.

3.1.2 Structural features of cathode surface and energy spectrum analysis

The surface topography of different cathodes shows that the gully on the surface of the blank carbon fiber was shallow and narrow (Fig.4a). The oxidized carbon fiber surface structure was completely maintained with the surface slightly etched and the gully was deep and wide (Fig.4b). After the CTS was grafted, a layer of thin film was formed on the surface of the carbon fiber and the partial region presented a protruding structure (Fig.4c). It can be seen from EDS analysis that elements C, N, O, Cl and Fe were found on the surface of the CTS-Fe^{3+}-modified cathode (Fig.5). Combined with FT-IR analysis, amide I, II and III bands were found on the surface of the carbon fiber, it is sure that the CTS-Fe^{3+}-modified cathode was successfully prepared by this method.

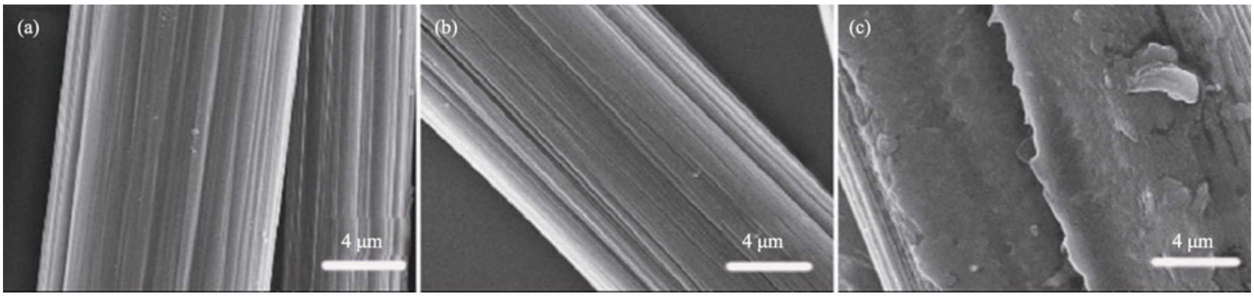

Fig.4 Surface patterns of cathode before and after modification. (a), blank carbon fiber; (b), nitric acid oxidation sample; (c), chitosan grafted sample.

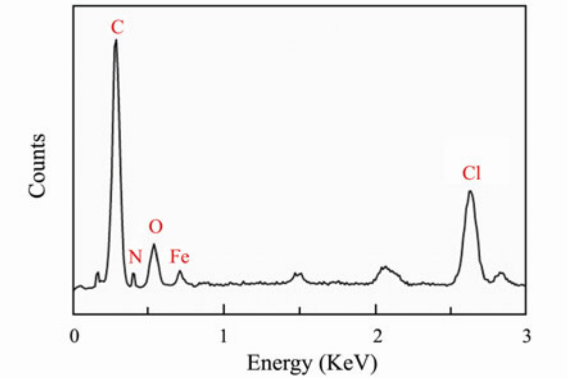

Fig.5 Energy dispersive spectrum for CTS-Fe^{3+} modified cathode surface.

Table 1 Energy dispersive spectrum data for CTS-Fe^{3+} modified cathode surface

Element	C	N	O	Cl	Fe	Total amount
Atomic (%)	80.157	0.700	15.598	2.707	0.838	100.000

3.2 Electrochemical Performance of Cathode

3.2.1 Cyclic voltammetry and cathode surface capacitance analysis

Different cyclic voltammetry (CV) curves for the cathodes are shown in Fig.6, in which no obvious oxidation and reduction peaks were found for the blank, O and CTS cathodes, presenting pure capacitance behavior. The specific capacitance of the CTS-modified sample was larger than that of the blank and O samples. For the CTS-Fe^{3+}-modified sample, the Fe^{2+}/Fe^{3+} oxidation peak occurred near 0.35 V (*vs*. Ag/AgCl) and the reduction peak near 0.54 V (*vs*. Ag/AgCl), meaning that the valence state conversion existed. According to the CV curves and the equation

$$C = \frac{1}{sA\Delta V}\int_{V_0}^{V_0+\Delta V} i\,\mathrm{d}V, \qquad (1)$$

where C is the specific capacity ($\mathrm{F\,g^{-1}}$), s is the scanning speed ($\mathrm{V\,s^{-1}}$), A is the quality (g), ΔV is the electric potential window and i is the electric current (mA).

The specific capacitances of the cathode was calculated and listed in Table 2. Their specific capacitances of O, CTS and CTS-Fe^{3+} were 9.2, 12.0 and 16.2 times larger than that of the blank respectively, among which the cyclic voltammetry specific capacitance of the CTS-Fe^{3+} group was the largest, meaning the chelation of CTS and Fe^{3+} increased the capacity of capturing and storing electrons effectively.

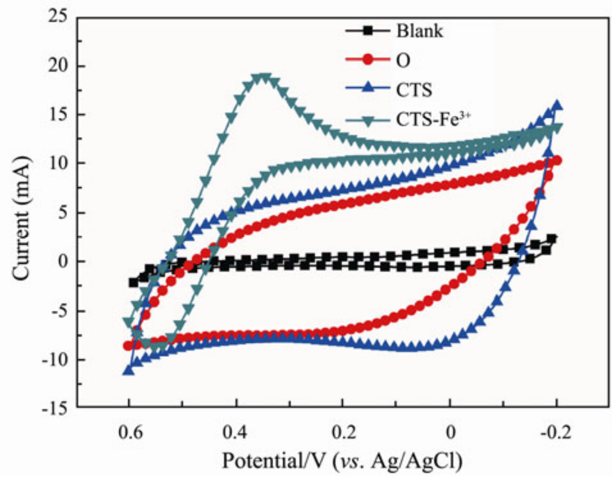

Fig.6 Different CV curves for different cathodes.

Table 2 CV curve parameters for different cathodes

Electrode	Blank	O	CTS	CTS-Fe^{3+}
S (V mA)	1.030	9.430	12.34	16.72
C ($\mathrm{F\,kg^{-1}}$)	73.950	677.07	886.01	1200.5

3.2.2 Analysis of Tafel curves and electron transfer kinetics of cathode

The exchange current density reflects the instant electron transfer kinetic activity at the interface between electrode and dissolved oxygen in sea water, the higher the exchange current density, the lower the reaction activation energy, the faster the redox reaction and the shorter time for the electrode reaching steady state. The Tafel test results for different cathodes have been shown in Fig.7 and the fitting results listed in Table 3. The exchange current densities of O, CTS and the CTS-Fe^{3+} groups were 5.2, 5.5 and 6.2 times larger than the blank group, respectively, meaning the kinetic activity of all modified cathodes increased significantly. The anti-polarization capacity was enhanced and the open-circuit potential of the modified cathode was significantly higher than that of the blank, with the maximum range reaching 138 mV for the

CTS-Fe^{3+}cathode. The electron transfer media were introduced from the complex of CTS and Fe^{3+}, the electric charge was transferred from the metal center with abundant electricity to the π* orbit of O_2 and the oxygen reduction activity was enhanced by weakened O-O bonds. Meanwhile, the conversion of Fe^{3+} and Fe^{2+} accelerated the oxygen reduction reaction, enhanced the cathode anti-polarization capability, and therefore, improved the electricity generation performance of the cell.

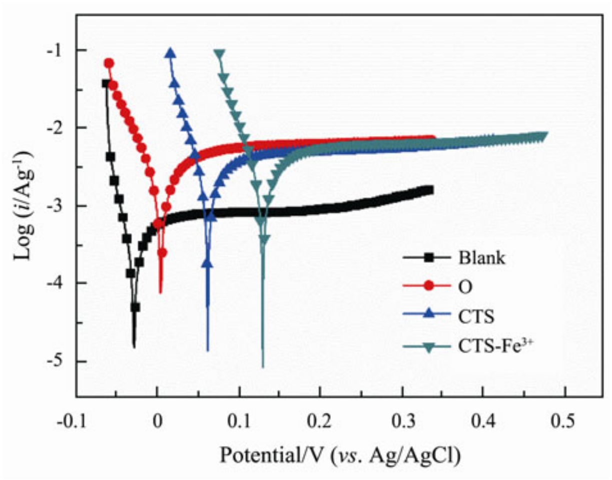

Fig.7 Tafel curves for different cathodes.

Table 3 Tafel curve parameters for different cathodes

Electrodes	OCP (V)	i_0 ($\times 10^{-4}$ A g^{-1})	KA
Blank	0.1390	6.417	1.0
O	0.1419	33.43	5.2
CTS	0.2169	35.00	5.5
CTS-Fe^{3+}	0.2770	40.00	6.2

Among them, the higher kinetic activity of O group should be attributed to the occurrence of higher amount of oxygen-containing groups after chemical oxidation treatment, such as, the carboxyl, carbonyl, and hydroxyl group (Liu *et al.*, 2019), which they will improve the dissolved oxygen reduction reaction (Fu *et al.*, 2014).

3.2.3 Polarization curve and its polarization performance

Cathode polarization is the phenomenon where the cathode potential is away from the balanced state when the electricity passed through the circuit. The main factors influencing cathode polarization were the ORR rate and its diffusion rate. Their polarization curves are given in Fig.8 and the anti-polarization capability was sequenced as CTS-Fe^{3+} > CTS > O > blank, among which the CTS-Fe^{3+} group was the best, with the largest exchange current density and best anti-polarization performance. These results were consistent with the CV curves (Fig.6) and Tafel curves (Fig.7).

In Fig.8, the shoot-back-up peaks in the polarization curves were caused by the grade shift of voltage and current in multimeter from mV to V and from mA to A respectively.

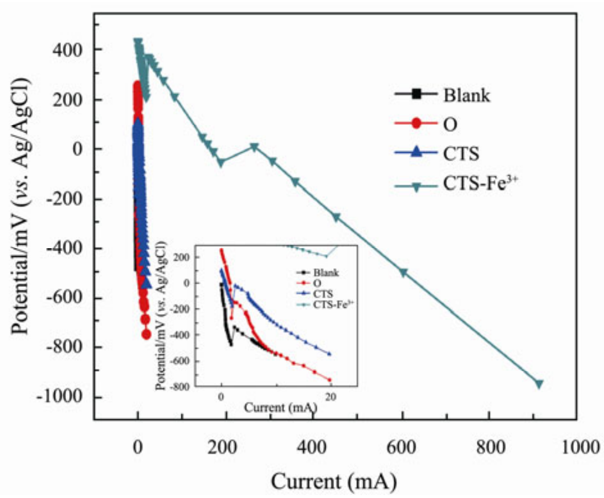

Fig.8 Different cathode polarization curves.

3.2.4 Impedance analysis

After the consecutive and steady discharging process, an electrochemical impedance analysis was conducted on the modified cathode. The result was fitted with Zview software and the fitting curves were obtained (Fig.9 and Table 4). For the CPE components, CPE-l-T and CPE-l-P represented the electrical double-layer capacitance and its deviation respectively, while W_R was the diffusion impedance, Rs the ohmic resistance and Rct the electron transfer resistance.

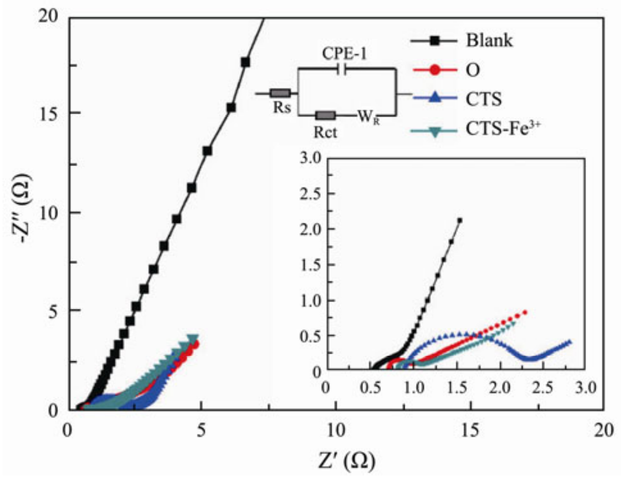

Fig.9 Different cathodic electrochemical impedance fitting curves.

Table 4 Electrochemical impedance fitting results

Electrode	Blank	O	CTS	CTS-Fe^{3+}
R_s (Ω)	0.5390	0.7252	0.8812	0.8308
CPE-1-T ($\times 10^{-4}\Omega^{-1}cm^{-2}s^{-n}$)	758.7	0.2839	9.604	0.3566
CPE-1-P ($\times 10^{-2}$)	73.49	124.0	81.64	121.1
R_{ct} (Ω)	0.5189	0.1472	1.334	0.1146
W_R (Ω)	209.0	6.681	2.222	2.849

It shows that the solution resistance R_s changed minimally after modification and the electron transfer resistance R_{ct} for the O and CTS-Fe^{3+} samples both decreased compared with the blank group, while the electron transfer resistance for CTS modification increased marginally, which should be attributed to thin film formation (Fig.3c), hindering the electron transfer. With the CTS-Fe^{3+} modification, Fe^{3+} on the cathode increases the electron transfer efficiency due to the valence conversion, so its electron transfer resistance decreased significantly. The CTS-Fe^{3+} complex received electron and became the Fe^{2+}-chitosan complex and Fe^{2+} was oxidized to Fe^{3+} by DO in seawater. In this process, the exchange current density at the cathode/seawater interface increased and the oxygen reduction kinetic improved greatly, which was in correspondence with the Tafel results (Fig.6 and Table 3).

3.3 Cell Power Performance

Maximum power output is an important parameter representing the MSMFCs performance. As shown in Fig.10, the maximum power output of cell from the CTS-Fe^{3+} group (613.0 mW m^{-2}) was 54 times greater than that from the blank group (11.4 mW m^{-2}) and the current output corresponding with maximum power output also increased by 56 times. The valence variation between Fe^{3+} and Fe^{2+} in the CTS-Fe complex as an electron transfer media accelerated the cathode oxygen reduction (Gong *et al.*, 2009; Asghar *et al.*, 2017), thereby improving the higher electricity generation in the MSMFCs.

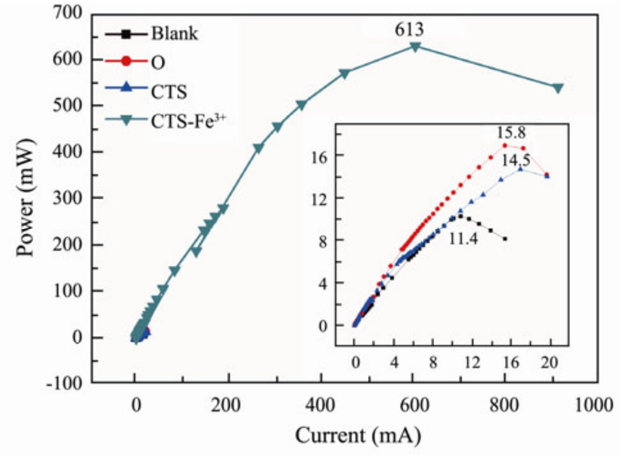

Fig.10 Different power curves for different MSMFCs.

The cell powers keep sustainable stability in three months and vary little with time and sea water temperature (Table 5).

Table 5 Cell powers output along with time and temperature in three months (mW m^{-2})

Time	Blank	O	CTS	CTS-Fe^{3+}	Sea water temp. (℃)
15 d	11.4	14.5	15.8	613	16
30 d	12.1	15.0	16.5	620	18
45 d	12.5	15.6	17.0	623	20
60 d	12.5	15.6	17.1	623	23

3.4 Mechanism Analysis

The cathode mechanism for the CTS-Fe^{3+}-modified carbon fiber is shown in Fig.11. The grafting of CTS makes carbon fiber have the coordination capability (Fig.11a), in which amino groups in the CTS molecules chelate with iron ions. After the cell loop was formed, electrons generated by bacteria on the anode surface in the sediments were transferred to the cathode from external electric circuit. The Fe^{3+} ions on the cathode surface captured electrons and converted into Fe^{2+}, which was instantly oxidized to Fe^{3+} by the dissolved oxygen in seawater. The CTS-Fe^{3+} complex was equivalent to high efficient DO redox catalysis, which could accelerate its reduction kinetics in seawater (Fig.11b).

The CTS-Fe^{3+} complex catalysis could be illustrated as follows: chelation of Fe^{3+} acts as an electron transfer media, in which the electric charge should be transferred from metal center with abundant electric charges to the π* orbit of O_2, weakening O-O bonds (Cavalcanti *et al.*, 2012; Zhang *et al.*, 2015) and finally improving the oxygen reduction kinetic activity. Therefore, cathode depolarization capability and the electricity generating performance of the cell were both improved, which can be

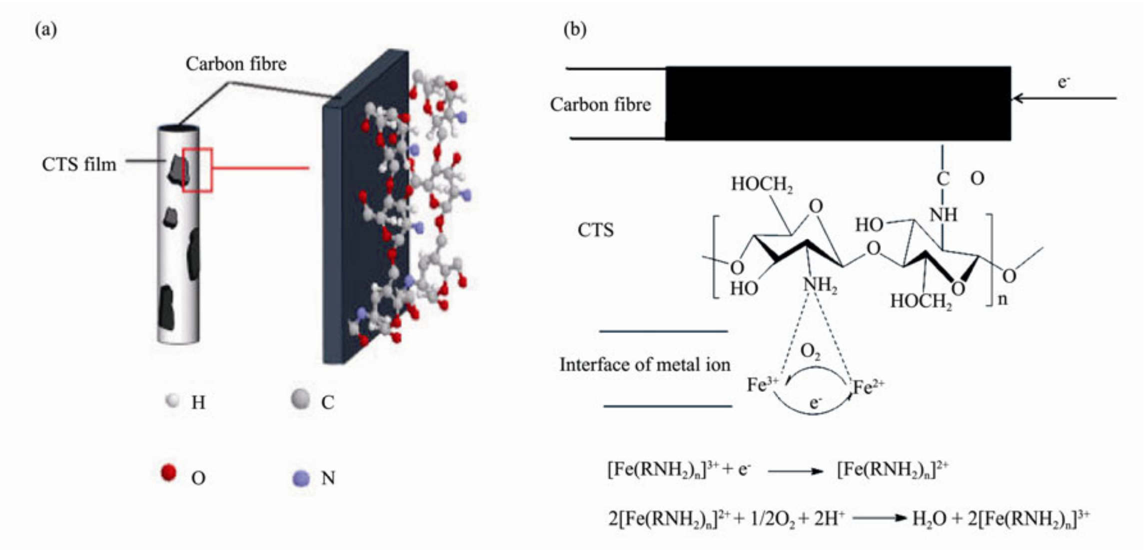

Fig.11 Cathode coordinative catalysis mechanism of dissolved oxygen reduction in seawater by the CTS-Fe^{3+} complex. (a), CTS grafting site on the carbon surface forming chelation ability of Fe ions. (b), CTS-Fe ion chelation accelerates dissolved oxygen reduction reaction.

proved by the electrochemical performance (Figs.7–9) and cell power output (Fig.10).

4 Conclusions

Chitosan existing naturally in the ocean has been grafted and chelated with iron ion onto the carbon fiber cathode, promoting the reduction kinetics of the dissolved oxygen in the sea-water, and significantly improving power output of MSMFCs, in which, its exchange current density for CTS-Fe^{3+} group is 6.2 times of that for blank, and the maximum increasing range of open circuit potential for CTS-Fe^{3+} group reaches 138 mV. The power output for CTS-Fe^{3+} group (613.0 mW m^{-2}) is 54 times bigger than that for blank, and the electric current output increases by 56 times.

The huge circulation of iron ions naturally existing in seawater have a significant biogeochemical effect (Yang *et al*., 2017), meanwhile, the high efficient ORR in seawater plays a vital role in maintaining the MSMFC. Therefore, this research creatively designs a high-efficient CTS-Fe ions modified cathode, which will be significant for a higher power and long-lasting MSMFCs.

Acknowledgement

This research is supported by the National Natural Science Foundation of China (No. 22075262).

References

Asghar, A., Raman, A. A. A., Daud, W. M. A. W., Ahmad, M., and Zain, S. U. B. M., 2017. Effect of nitrogen doping on graphite cathode for hydrogen peroxide production and power generation in MFC. *Journal of the Taiwan Institute of Chemical Engineers*, **76**: 89-100, DOI: 10.1016/j.jtice.2017.04.016.

Asim, A. Y., Mohamad, N. M. I., and Susana, R. C., 2020. Development and modification of materials to build cost-effective anodes for microbial fuel cells (MFCs): An overview. *Biochemical Engineering Journal*, **164**: 107779, DOI: 10.1016/j.bej.2020.107779.

Babauta, J. T., Hsu, L., Atci, E., Kagan, J., Chadwick, B., and Beyenal, H., 2014. Multiple cathodic reaction mechanism in seawater cathodic biofilms operating in sediment microbial fuel cell. *ChemSusChem*, **7** (10): 2898-2906, DOI: 10.1002/cssc.201402377.

Cavalcanti, I. T., Silva, B. V. M., Peres, N. G., Moura, P., Sotomayor, M. D. P. T., Guedes, M. I. F., *et al*., 2012. A disposable chitosan modified carbon fiber electrode for dengue virus envelope protein detection. *Talanta*, **91**: 41-46, DOI: 10.1016/j.talanta.2012.01.002.

Chen, W., Liu, Z. H., Su, G., Fu, Y. B., Zai, X. R., Zhou, C. Y., *et al*., 2017. Composite-modified anode by MnO_2/polypyrrole in marine benthic microbial fuel cells and its electrochemical performance. *International Journal of Energy Research*, **41** (6): 845-853, DOI: 10.1002/er.3674.

Cheng, L., Reimers, C. E., and Alleau, Y., 2020. Inducing the attachment of the cable bacteria on oxidizing electrodes. *Biogeosciences Discussions*, **17** (3): 597-207, DOI: 10.5194/bg-17-597-2020.

Ewing, T., Ha, P. T., and Beyenal, H., 2017. Evaluation of long-term performance of sediment microbial fuel cells and the role of natural resources. *Applied Energy*, **192**: 490-497, DOI: 10.1016/j.apenergy.2016.08.177.

Fu, Y. B., Liu, Y. Y., Xu, Q., Lu, Z. K., and Zhang, Y. L., 2014. Comparative study of two carbon fiber cathodes and theoretical analysis in microbial fuel cells on ocean floor. *Journal of Ocean University of China*, **13** (2): 257-261, DOI: 10.1007/s11802-014-2162-z.

Gajda, I., Greenman, J., Santoro, C., Serov, A., Melhuish, C., Atanassov, P., *et al*., 2018. Improved power and long term performance of microbial fuel cell with Fe-NC catalyst in air-breathing cathode. *Energy*, **144**: 1073-1079, DOI: 10.1016/j.energy.2017.11.135.

Ge, J. G., Yue, P. X., Chi, J. P., Liang, J., and Gao, X. L., 2018. Formation and stability of anthocyanins-loaded nanocomplexes prepared with chitosan hydrochloride and carboxymethyl chitosan. *Food Hydrocolloids*, **74**: 23-31, DOI: 10.1016/j.foodhyd.2017.07.029.

Ghoreishi, K. B., Ghasemi, M., Rahimnejad, M., Yarmo, M. A., Daud, W. R. W., Asim, N., *et al*., 2014. Development and application of vanadium oxide/polyaniline composite as a novel cathode catalyst in microbial fuel cell. *International Journal of Energy Research*, **38** (1): 70-77, DOI: 10.1002/er.3082.

Gong, K., Du, F., Xia, Z., Durstock, M., and Dai, L., 2009. Nitrogen-doped carbon nanotube arrays with high electrocatalytic activity for oxygen reduction. *Science*, **323** (5915): 760-764, DOI: 10.1126/science.1168049.

Huang, H., Cheng, S., Yang, J., Li, C., Sun, Y., and Cen, K., 2018. Effect of nitrate on electricity generation in single-chamber air cathode microbial fuel cells. *Chemical Engineering Journal*, **337**: 661-670, DOI: 10.1016/j.cej.2017.12.150.

Jiang, Y., Zhai, Q., Guo, H., Tan, H., and Guo, S. Y., 2007. Coordination characteristics of chitosan on Zn/Fe ions and the application of the coordination compounds. *Modern Food Science and Technology*, **23** (9): 88-92 (in Chinese with English abstract).

Liu, A., Fu, Y. B., Zai, J. Z., Duan, Z. W., and Zai, X. R., 2019. Electrochemical and electric field response properties of highly sensitive electrodes based on carbon fiber with oxygen and nitrogen groups. *IEEE Sensors Journal*, **19**: 3966-3974, DOI: 10.1109/JSEN.2019.2891905.

Liu, W., Cheng, S., Yin, L., Sun, Y., and Yu, L., 2018. Influence of soluble microbial products on the long-term stability of air cathodes in microbial fuel cells. *Electrochimica Acta*, **261**: 557-564, DOI: 10.1016/j.electacta.2017.12.154.

Mahmoud, M. S., Wen, B., Su, Z., Fan, S., and Zhang, Y., 2018. Parameters influencing power generation in eco-friendly microbial fuel cells. *Paper and Biomaterials (PBM Microbial Fuel Cells)*, **3** (1): 10-16.

Ngoc, B. D., Chih-Liang, W., Li, Z., Wan, T., and Hsiharng, Y., 2019. Development of a facile and low-cost chitosan modified carbon cloth for efficient self-pumping enzymatic biofuel cells. *Journal of Power Sources*, **429**: 111-119, DOI: 10.1016/j.jpowsour.2019.05.001.

Son, E. B., Poo, K. M., Mohamed, H. O., Choi, Y. J., Cho, W. C., and Chae, K. J., 2018. A novel approach to developing a reusable marine macroalgae adsorbent with chitosan and ferric oxide for simultaneous efficient heavy metal removal and easy magnetic separation. *Bioresource Technology*, **259**: 381-387, DOI: 10.1016/j.biortech.2018.03.077.

Song, X., Liu, J., Jiang, Q., Qu, Y., He, W., Logan, B., *et al*., 2018. Enhanced electricity generation and effective water filtration using graphene-based membrane air-cathodes in microbial fuel cells. *Journal of Power Sources*, **395**: 221-227, DOI: 10.1016/j.jpowsour.2018.05.043.

Tender, L., Gray, S., Groveman, E., Lowy, D., Kauffman, P., Melhado, J., *et al*., 2008. The first demonstration of a microbial fuel cell as a viable power supply: Powering a meterological buoy. *Journal of Power Sources*, **179** (2): 571-575, DOI: 10.1016/j.jpowsour.2007.12.123.

Wang, B., Zhang, H., Yang, Y. G., and Xu, M. Y., 2021. Diffusion and filamentous bacteria jointly govern the spatiotemporal process of sulfide removal in sediment microbial fuel cells. *Chemical Engineering Journal*, **405**: 126680, DOI: 10.1016/j.cej.2020. 126680.

Wu, S., He, W., Yang, W., Ye, Y., Huang, X., and Logan, B., 2017. Combined carbon mesh and small graphite fiber brush anodes to enhance and stabilize power generation in microbial fuel cells treating domestic wastewater. *Journal of Power Sources*, **356**: 348-355, DOI: 10.1016/j.jpowsour.2017.01.041.

Yang, H., Gong, L., Wang, H., Dong, C., Wang, J., Qi, K., *et al*., 2020. Preparation of nickel-iron hydroxides by microorganism corrosion for efficient oxygen evolution. *Nature Communication*, **11** (1): 5075-5083, DOI: 10.1038/s41467-020-18891-x.

Yang, J., RyeolKim, H., HyunLee, J., UkLee, H., and WookKim, S., 2021. Electrochemical properties of enzyme electrode covalently immobilized on graphite oxide/cobalt hydroxide/chitosan composite mediator for biofuel cells. *International Journal of Hydrogen Energy*, **46** (4): 3251-3258, DOI: 10.1016/j.ijhydene.2020.03.084.

Yang, R. J., Su, H., Qu, S. L., and Wang, X. C., 2017. Capacity of humic substances to complex with iron at different salinities in the Yangtze River Estuary and East China Sea. *Scientific Reports*, **7** (1): 1381-1390, DOI: 10.1038/s41598-017-01533-6.

Zhang, H. S., Fu, Y. B., Zhou, C. Y., Liu, S., Zhao, M. G., Chen, T. L., *et al*., 2018. A novel anode modified by 1, 5-dihydroxyanthraquinone/multiwalled carbon nanotubes composite in marine sediment microbial fuel cell and its electrochemical performance. *International Journal of Energy Research*, **42** (7): 2574-2582, DOI: 10.1002/er.4034.

Zhang, J., Chen, N., Tang, Z., Yu, Y., Hu, Q., and Feng, C., 2015. A study of the mechanism of fluoride adsorption from aqueous solutions onto Fe-impregnated chitosan. *Physical Chemistry Chemical Physics*, **17** (18): 12041-12050, DOI: 10.1039/c5cp00817d.

Zhao, Q., Ji, M., Li, R., and Ren, Z., 2017. Long-term performance of sediment microbial fuel cells with multiple anodes. *Bioresource Technology*, **237**: 178-185, DOI: 10.1016/j.biortech.2017.03.002.

Zhou, C. Y., Fu, Y. B., Zhang, H. S., Chen, W., Liu, Z., Liu, Z. H., *et al*., 2018 Structure design and performance comparison of large-scale marine sediment microbial fuel cells in lab and real sea as power source to drive monitoring instruments for long-term work. *Ionics*, **24**: 797-805, DOI: 10.1007/s11581-017-2251-2.

Zhou, X., Xu, Y., Mei, X., Du, N., Ju, R., Hu, Z., *et al*., 2018. Polyaniline/β-MnO_2 nanocomposites as cathode electrocatalyst for oxygen reduction reaction in microbial fuel cells. *Chemosphere*, **198**: 482-491, DOI: 10.1016/j.chemosphere.2018.01.058.

(Edited by Ji Dechun)